ACS Sustainable Chemistry & Engineering

pubs.acs.org/journal/ascecg

Research Article

Upcycling Orange Peel Agricultural Waste for the Preparation of Green Hydrogels as Active Soil Conditioners

Danila Merino,* Andrea Yamila Mansilla, María Florencia Salcedo, and Athanassia Athanassiou*

Cite This: https://doi.org/10.1021/acssuschemeng.3c02992

Read Online

ACCESS | Metrics & More | Article Recommendations | Supporting Information

ABSTRACT: In this work, agar (Aa)-based hydrogels were developed incorporating different concentrations of orange peel (OP) particles, pretreated using three different methods (hydrolysis, ultrasonication, or simple suspension in hot water), and 1.5 wt % limonene (LMN), to be tested as active soil conditioners for agriculture. The results of swelling of these hydrogels in distilled and tap water showed that acid hydrolysis or ultrasonication pretreatments of OP are counterproductive and that the simplest and lowest-energy method of OP pretreatment resulted in the most efficient hydrogels in terms of swelling. The incorporation of LMN into the Aa-based hydrogels increased their swelling capacity in tap water, while the incorporation of OP particles in the Aa+LMN hydrogels increased the number and decreased the size of their pores but did not significantly influence their swelling capacity, which ranged from 650 to 700% after 4 h of immersion. The hydrogels developed here were prepared with up to 50 wt % OP particles due to the increased water solubility for higher concentrations. The biopesticide activity of the hydrogels was investigated against the bacterium *Pseudomonas syringe* pv *tomato* DC3000 (*Psy*) and the necrotrophic fungus *Fusarium solani* f. sp. eumartii (*F. eumartii*), while the ability of the hydrogels as soil conditioners to retain soil moisture under simulated drought conditions was exploratorily investigated in tomato plants. The results demonstrate that even if the hydrogels did not show biopesticide activity against the studied microorganisms, the addition of 2.5 wt % hydrogel to the substrate significantly increased the moisture content of the soil and consequently improved the relative water content of tomato leaves under drought stress.

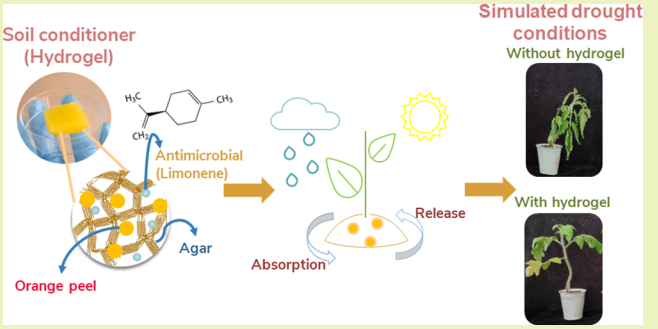

KEYWORDS: *Sustainable agriculture, fertilizer, food waste, soil substrate moisture*

INTRODUCTION

Water scarcity, soil quality degradation, biodiversity loss, and high levels of greenhouse gas emissions indicate that the current agricultural system is not sustainable and is compromising the future of our planet.[1,2] Simultaneously, and in agreement with the Sustainable Development Goal (SDG) number two of the United Nations, UN SDG2: "Zero Hunger", significant and sustainable agricultural productivity increments must occur in the following years to meet the food demand of a growing world population.[2,3]

Rendering current agricultural systems to be highly efficient and sustainable is an enormous and complex challenge that can be faced in many different ways. Some emerging materials that have huge potential for that purpose are soil conditioners. In general, soil conditioners are materials that can enhance crop yields while preserving soil structure and nutrients and ensuring water retention. Among the materials described in the literature, hydrogels seem the most promising at addressing this task.[4−6] They are three-dimensional cross-linked polymer networks that can incorporate large amounts of water in their structure and release that water depending on surrounding conditions and plants' demands.[7,8] The use of hydrogels contributes to more efficient management of irrigation water and increases the water retention capacity of the soil and its porosity, providing plants with moisture and a conducive atmosphere for root development, all parameters that ultimately increase crop yields.[9,10]

Commercial hydrogels intended for this application are based on polyacrylate or polyacrylamide polymers, which are petroleum-derived and nonbiodegradable. In recent decades, great scientific efforts have been dedicated to the replacement of these hydrogels with biodegradable alternatives.[6] However, in many cases, acrylates and acrylamide monomers are still being used as cross-linkers of polymer molecules, and issues such as the hydrogels' incomplete degradability with the consequent generation of micro- or nanoplastics are still unresolved.[4,11−13] Therefore, this work aims to provide an

Received: May 19, 2023
Revised: June 28, 2023

Table 1. Samples' Name and Composition

sample name	volume Aa 1.5 wt % (mL)	volume yOP[a] 1.5 wt % (mL)	volume LMN 1.5 wt % (mL)	OP content with respect to Aa (wt %)	final LMN content in Aa hydrogels (wt %)
Aa	20.00	-	-	-	-
Aa+LMN	19.70	-	0.30	-	1.5
Aa+10%yOP	18.00	2.00	-	10	-
Aa+20%yOP	16.00	4.00	-	20	-
Aa+30%yOP	14.00	6.00	-	30	-
Aa+40%yOP	12.00	8.00	-	40	-
Aa+50%yOP	10.00	10.00	-	50	-
Aa+10%yOP +LMN	17.73	1.97	0.30	10	1.5
Aa+20%yOP +LMN	15.76	3.94	0.30	20	1.5
Aa+30%yOP +LMN	13.79	5.91	0.30	30	1.5
Aa+40%yOP +LMN	11.82	7.88	0.30	40	1.5
Aa+50%yOP +LMN	9.85	9.85	0.30	50	1.5

[a]y = h, s, or p.

active and sustainable alternative to these hydrogels by utilizing all-natural biodegradable compounds, upcycling industrial vegetable waste. Such an approach also contributes to the circular economy principle included in the UN SDG 12: "Responsible consumption and production".[14,15]

Thanks to its excellent gelling properties and ease of large scale scalability, the agar (Aa) polymer was chosen as the matrix for preparing the active hydrogels. The hydrogels were loaded with orange peel (OP) and *R*-(+)-limonene (LMN), a widely known biopesticide.[16−19] The Aa polymer is a hydrocolloid extracted from the *Gelidiaceae* and *Gracilariaceae* families of seaweeds, and it is composed of two polysaccharides, agarose and agaropectin, with agarose being the major component and responsible for the gelling properties.[20] Agar hydrogels stand out because of their thermoreversibility, since they become liquid above their melting temperature of ∼85−95 °C, and they form gels when cooled (gel point ∼32−45 °C) by the formation of hydrogen bonds between their molecules.[20] The gelation process is guided by the arrangement of agarose molecules in simple or double helices followed by the supramolecular arrangement of these in a macroreticulum.[21] This polymer has applications in the food, pharmaceutical, cosmetic, textile, paper, and biotechnology industries as stabilizer, thickener, emulsifier, and filler.[20] Besides, it is "Generally Recognized as Safe" (GRAS) by the Food and Drug Administration (FDA) and approved as a food additive by the European Food Safety Authority (EPSA).[20,22]

On the other hand, the orange fruit is the most consumed citrus and represents 60% of world citrus production. In 2020 alone, more than 75 million tons of oranges were produced worldwide, of which 18% were used for the industrial production of juice, which generates OP as the main byproduct, representing approximately 45% of the total mass processed.[23−25] OP is rich in several active compounds such as polyphenols, essential oils, flavonoids, micro- and macronutrients, and the polymer pectin, a complex heteropolysaccharide composed of 1,4-linked α-D-galacturonate residues, some of which are esterified to form methyl esters.[26] Interestingly, the orange essential oil is mainly composed of LMN. This compound has several valuable properties in agriculture, such as insect-repellent and biopesticide properties, so it was added to the hydrogels' formulation as an extra component that can potentially enhance the plants' protection against diseases.[16−19] However, special attention was paid to the concentration applied (1.5 wt %) to avoid phytotoxic effects.[19,27] It is important also to mention that LMN has low toxicity to human beings and has also been reported to have antitumor, antioxidant, and anti-inflammatory activity.[28]

In this work, different OP pretreatments were conducted to identify the best way to combine OP with Aa. For that, powdered OP particles were either hydrolyzed in acidic media (hOP), treated with ultrasound (sOP), or added without further treatment to hot water (pOP) before being introduced to the Aa solution. The hydrogels obtained from the combination of hOP, sOP, or pOP, and Aa or Aa + LMN were physicochemically characterized, and their swelling capacity and water solubility were evaluated in distilled and tap water. In vitro testing of the optimal formulation as a biopesticide against the bacteria *Psy* and the fungus *F. eumartii* revealed no biopesticide action. Besides, the effect of the best hydrogel formulation on tomato plant growth was evaluated in simulated drought conditions, providing clear evidence for its application in horticultural systems.

EXPERIMENTAL SECTION

Materials. Microbiological grade agar powder, *R*-(+)-limonene, and Tween 80 were purchased from Sigma-Aldrich. Dried OPs (*C. sinensis*) supplied from PepsiCo (Milan, Italy) were kept in a polyethylyne bag until used. For antimicrobial assays, *Psy* (NCPPB, collection no. 1008), a well characterized Gram-negative bacterium, was used. The bacterium was maintained on King's B (KB) agar medium[29] containing suitable antibiotics, 50 μg mL^{-1} rifampicin and 50 μg mL^{-1} kanamycin, according to Mansilla et al.[30] Single colonies grown at 30 °C for 48 h were isolated, transferred to KB broth, and grown overnight at 30 °C with shaking. *F. eumartii* was obtained from the Estación Experimental Agropecuaria (EEA), Instituto Nacional de Tecnología Agropecuaria (INTA), Balcarce, Argentina. Spores were harvested from 8-day-old cultures grown on solid potato dextrose agar (PDA) medium at 25 °C by adding 1 mL of sterile water to the plates and scraping the surface. Conidia were counted using a hemocytometer, diluted to the appropriate concentration, and used for the assay.

OP Preteatments. First, OP was ground in a dry-mill-IKA-Pilotina MC (Germany) to a particle size < 250 μm. Then, suspensions of OP powder were prepared by three different methodologies: acid hydrolysis (hOP), ultrasonication (sOP), and

https://doi.org/10.1021/acssuschemeng.3c02992
ACS Sustainable Chem. Eng. XXXX, XXX, XXX−XXX

simple powder suspension in hot water (pOP). For hOP preparation, 1.5 g of OP was added into 100 mL of 1 M acetic acid. The suspension was stirred at 700 rpm and heated at 30 °C during 24 h. The sOP suspension, on the other hand, was prepared in the same concentration as hOP but in distilled water. Ultrasonication was done in an Ultrasonic tip SONICS Vibra-Cell (United States) by applying ten pulses of 30 s at 40% amplitude with intervals of 30 s. Finally, pOP suspension was prepared by adding 1.5 g of OP into 100 mL of distilled water and stirring the solution at 90 °C and 500 rpm during 15 min.

LMN Nanoemulsion Preparation. The nanoemulsion was prepared as reported by de Castro e Silva et al. with some modifications.[31] LMN nanoemulsion at 1.5 wt % was prepared by adding 0.75 g of LMN in 50 mL of distilled water. Tween 80 was also added as emulsifier in a 0.5 wt % with respect to the LMN. The nanoemulsion was prepared by ultrasonication in an Ultrasonic tip SONICS Vibra-Cell TM (United States) by applying 4 pulses of 30 s at 40% with intervals of 30 s. Particle size and Z-potential were measured by dynamic light scattering (DLS) in a MALVERN Nano ZS (United Kingdom) instrument, and they were 312 nm and −30.4 mV, indicating that the nanoemulsion was stable.[32]

Preparation of Hydrogels. Hydrogels were prepared by combining different amounts of hOP, sOP, or pOP (10−50 wt %) with Aa or Aa + LMN. For that, a 1.5 wt % Aa aqueous solution was prepared by dissolving it under heating at 90 °C and stirring at 500 rpm during 1 h. After that, the hydrogels were prepared by the combination of different aliquots of 1.5 wt % Aa, 1.5 wt % LMN, and 1.5 wt % OP solutions (Table 1).

Therefore, Aa-based gels were prepared with 10, 20, 30, 40, and 50 wt % of OP (hOP, sOP, or pOP) with or without the addition of 1.5 wt % of LMN. The resulting composites were stirred for 30 min at 90 °C, and then they were placed in Petri dishes at room temperature to allow them to gel and dry. After 48 h, they were dried in a vacuum oven at 30 °C overnight and stored in sealed PE bags until their use. Samples were labeled as "Aa + *x*% yOP" or "Aa + *x*% yOP + LMN", where *x* = 10, 20, 30, 40, or 50 is the OP content with respect to Aa (wt %), and y = h, s, or p, where h stands for "hydrolyzed", s for "sonicated", and p for "particles". The samples "Aa" and "Aa + LMN" were also prepared as controls, and they were 100% Aa solution or 98.5 wt % Aa and 1.5% LMN nanoemulsion, respectively. For the biological tests, the hydrogels were ground with an Oster Versa 1400 blender to an average particle size of 300 μm.

Characterization of Hydrogels. *Fourier Transform Infrared Spectroscopy (FTIR).* FTIR spectra were recorded in a VERTEX 70v Bruker spectrometer (Germany) with an evacuable optics bench, which allows better sensitivity, and by using the attenuated total reflectance (ATR) tool with the diamond crystal accessory. The spectra were carried out in the 4000−600 cm^{-1} range, at a resolution of 4 cm^{-1} and with an average of 64 scans.

Thermogravimentric Analysis (TGA). TGA analysis was performed on a TA-Q500 instrument (United States). Samples were placed in platinum pans and heated from room temperature to 600 °C at 10 °C/min in a 50 mL/min flow of nitrogen.

Scanning Electron Microscopy (SEM). For hydrogel microstructure observation, samples were first swollen during 24 h in tap water and then freeze-dried during another 24 h. For that a CHRIST Epsilon 2−4 LSCplus liophilizer (Germany) was used at 10 °C and 1.14 mbar. Once dried, the samples were cryofractured by immersion in liquid nitrogen. After that, the cryofracture zone was attached to aluminum stabs with conductive carbon tape, and then they were covered with 10 nm of gold by sputtering. The microscope used for their observation was a JEOL JSM-6490LA (Japan) and was operated at 10 kV and 78 μA, using the secondary electrons (SEI) detector. Images were taken at 500, 2500, and 5000×.

Swelling Behavior in Different Media. The water absorption capacity of hydrogels was determined from the mass change before and after dipping a dried sample in specific media. For that, samples were dried in a vacuum oven at 40 °C overnight and cut in pieces of 1 cm × 1 cm. After that, their initial weight was recorded (W_i) in an analytical balance (Sartorious CPA225D). Then, they were submerged in distilled or tap water (mineral composition obtained by ICP: 0.055 ppm Al, 0.034 ppm B, 51.9 ppm Ca, 1.95 ppm K, 6.6 ppm Mg, and 18.1 ppm Na) during 24 h at room temperature (20 °C). The swollen samples were then removed, carefully dried using tissue paper, and weighed (W_f). The swelling percentage of the samples was determined using eq 1.

$$\text{swelling}\ (\%) = \frac{W_f - W_i}{W_i} \times 100\% \quad (1)$$

The swelling vs time curves of selected hydrogels were also determined. For that, the same procedure used for the swelling determination was followed, but the samples were periodically weighed during 24 h. The percentage of swelling was finally calculated by using eq 2.

$$\text{swelling}\ (\%) = \frac{W_t - W_i}{W_i} \times 100\% \quad (2)$$

where W_t is the weight of the sample at time t, and W_i is the weight of the dried sample at the beginning of the experiment. Finally, the effects of five cycles of swelling and deswelling on the swelling capacity of the hydrogels were also studied. For that, samples were swelled in tap water during 24 h, and then dried in a vacuum oven during 24 h at 40 °C and reswelled. The swelling in each cycle was calculated as indicated in eq 1. All samples were analyzed in duplicate, and the results were informed as the average ± standard deviation (SD).

Water Solubility (WS). WS gives an indication of the hydrogel water resistance. For its determination, the weighed samples were soaked in distilled water for 24 h, and subsequently, they were removed and dried in a vacuum oven at 40 °C for 24 h. Their final weight was recorded, and the WS was calculated using eq 3.

$$\text{WS} = \frac{W_f - W_i}{W_i} \times 100\% \quad (3)$$

where W_f is the final dry weight of the hydrogels, and W_i is the dry weight at the beginning of the experiment. All samples were analyzed in duplicate, and the results are presented as average ± SD.

Biopesticide Activity against Psy and F. eumartii. The antibacterial action of the best formulation of hydrogels was evaluated through quantification of the optical density (OD_{600}) of *Psy*cultures. For this, aliquots of overnight starter cultures of *Psy* were inoculated into fresh KB liquid medium to nearly 106 cells mL^{-1} and mixed with different concentrations of hydrogels as indicated. The control conditions were the bacterial inocula without hydrogels. After 24 h of exposure, the OD_{600} was measured using a GeneQuant 1300 spectrophotometer (Freiburg, Germany). Three independent tests with two replicates each were carried out.

The antifungal activity of the best hydrogels against *F. eumartii* spores was evaluated as described by Mendieta et al.[33] *F. eumartii* spores (1×10^6 spores/mL) were treated with different concentrations of hydrogels suspensions in a final volume of 50 μL of 1% sucrose and put on microslides. The spores of *F. eumartii* were incubated at 25 °C for 24 h in darkness. Germinated spores were visualized under a Nikon light microscope Eclipse E200 (Japan). Two independent tests with two replicates each were carried out.

Effect of Soil Conditioners on Tomato Plants Subjected to Water Stress. Tomato plants (*S. lycopersicum*, cv. Platense) were germinated in pots containing Grow Mix Multipro commercial substrate (Terrafertil, Argentina) and grown in culture chambers at 25 °C with 16:8 h light:dark during 18 days with daily irrigation.

In order to assess the effectiveness of hydrogels as soil conditioners under drought conditions, 0.5 or 2.5 wt % hydrogels were added individually to each pot. In the 3 days following supplementation with the conditioner, the seedlings were irrigated with mains water up to field capacity, and from that moment (21-day-old plants), irrigation was suspended. There were two control treatments. Plants grown in substrate without hydrogel supplements and under water stress (control without irrigation) were called control "C", and the plants grown in substrate without hydrogels supplement but with constant

https://doi.org/10.1021/acssuschemeng.3c02992
ACS Sustainable Chem. Eng. XXXX, XXX, XXX−XXX

irrigation were referred as control "CW". On day 4 of water stress, plants were rewatered with the volume of water necessary to reach 50% field capacity of the C plants to achieve mild drought stress.

Moisture content and water retention (WR) in each substrate were monitored during the 7 days of the water stress treatment. The moisture content was measured with a soil sensor (TFA-481000, Germany). Briefly, to determine the soil moisture, the probe tip was collocated into the substrate between the edge and the center of the pot to a depth of up to about 3/4 of the probe tip length. The scale is defined in arbitrary units, with a range from 0 to 10, where 0 indicates a dry substrate and 10 is the maximum moist substrate. Water retention was measured by weighing the pots every day and calculated as described in Jamnongkan et al.[34] using eq 4:

$$\mathrm{WR}\ (\%) = \frac{W_t - W}{W_0 - W} \times 100\% \tag{4}$$

where W_0 represents the total weight of each pot at field capacity, W_t represents the weight of the pot at time t, and W represents the weight of the pot containing the dry substrate.

On day 6 of the suspension of irrigation (27-day-old plants), the chlorophyll content was quantified using the Clorofilog manual detector (Falker, Brazil). At the end of the trial, after 7 days of water stress, the fresh weight (FW) and dry weight (DW) of the 28-day-old tomato plants were quantified. For this, the aerial part of the plants was cut and weighed on a digital scale before and after drying in an oven (Traveler Ohaus, China).

Finally, the leaf relative water content (RWC) was determined, since this parameter is an important indicator of water status in plants.[35] For this, fully expanded leaf discs from plants cultivated under each of the treatments were analyzed. Each sample was weighed in a vial (W_F) and then hydrated in water to ensure maximum turgor for approximately 3−4 h under light and room temperature. After hydration, the leaf discs were dried on filter paper and immediately weighed to estimate the weight of the maximum turgor (W_T). Then they were dried in an oven until constant weight, and the dry weight (W_D) was determined. The RWC (%) was calculated using eq 5:

$$\mathrm{RWC}\ (\%) = \frac{W_F - W_D}{W_T - W_D} \times 100\% \tag{5}$$

Biodegradation in Soil. The biodegradability of the most promising hydrogel was analyzed over a three month-experiment following the methodology reported by Merino et al.[36] Circular samples of 1 cm diameter were dried in a vacuum oven for 24 h at 40 °C, and weighed (W_0). After that, they were put into a PE-mesh bag and buried in the biodegradation media (VIGORPLANT ITALIA S.R.L., Fombio, Italy). This soil was composed of acidic sphagnum peat, composted, and noncomposted plant materials. At the beginning of the experiment, the soil was watered to half its holding capacity, and its humidity was maintained during the experiment, compensating the evaporated water with periodical water additions. The assay was conducted indoors. The average temperature was 20 ± 2 °C, and the average relative humidity was 60 ± 5% RH.

Samples were removed on days 5, 15, 30, and 60, and the soil attached to the samples was carefully removed with a brush. Unburied samples were dried overnight in a vacuum oven at 40 °C and reweighed (W_t). The weight loss (%) of each sample was determined, as shown in eq 6.

$$\text{weight loss}\ (\%) = (W_0 - W_t)/W_0 \times 100\% \tag{6}$$

Three replicates of each sample were analyzed, and the results were represented as the average ± SD as a function of time (days).

Statistical Analysis. Results were reported as mean ± SD. Furthermore, one-way analysis of variance (ANOVA) with Dunnet or Tukey's test was conducted in the Origin 2019b and GraphPad Prism version 5.01 software to determine if significant differences are found among mean values at a 0.05 level of significance.

RESULTS AND DISCUSSION

Physicochemical Characterization of Hydrogels. Characterization techniques such as FTIR, TGA, and SEM were employed to understand the interactions between pretreated OP particles, LMN, and Aa.

The FTIR spectra of Aa and Aa+LMN hydrogels are included in Figure S1. As expected, the Aa hydrogel (Figure S1a) presented only the typical bands of the agar polymer, in agreement with the literature.[37] The broad band appearing in the 3600−3000 cm^{-1} range is attributed to the stretching of −OH groups and is followed by several overlapped bands, of which at least the two more intense are centered at 2922 and 2854 cm^{-1} and attributed to the symmetric and asymmetric stretches of the hydrogen atoms in $-CH_2$ groups. Then, moving to the fingerprint region of the spectra, typical agar bands appeared at 1370 cm^{-1} due to the ester sulfate groups and at 1039 and 931 cm^{-1} due to the C−O stretching of the of 3,6-anhydro-galactose residues. Finally, the band centered at 886 cm^{-1} was attributed to the C−H stretching of the residual carbons of β-galactose.[37]

After the addition of LMN (Figure S1b) the bands found in the 3000−2850 cm^{-1} range, attributed to the symmetric and asymmetric stretching vibrations of C−H in $-CH_2$ and $-CH_3$ groups, increased their intensity. For instance, the ratio of intensities between the band centered at 2922 cm^{-1} (stretch of CH in $-CH_2$) and the one at 1039 cm^{-1} (stretch C−O−C in the glycosidic bonds and the ring) was 0.47 for Aa+LMN, while it was only 0.13 for Aa. This trend is in agreement with the presence of new apolar groups from LMN and the surfactant used to prepare its emulsion.

After the addition of OP in its different forms, the FTIR spectra of Aa and Aa+LMN changed significantly (Figure 1 and Figure S2, respectively). As an example, Figure 1 shows the FTIR spectra of the hydrogels obtained with Aa and 30 wt % of hOP (Figure 1c), sOP (Figure 1d), and pOP (Figure 1e). Besides, the FTIR spectra of raw OP particles (Figure 1a) and Aa (Figure 1b) are also included as controls to better understand the changes observed.

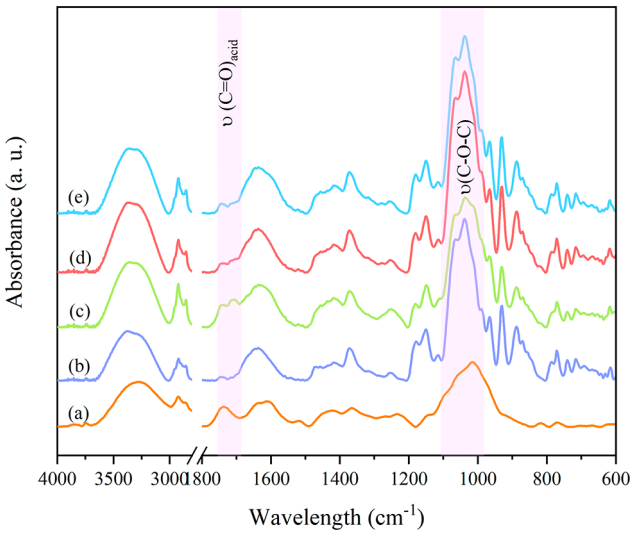

Figure 1. FTIR spectra of (a) OP, (b) Aa, (c) Aa+30hOP, (d) Aa +30sOP, and (e) Aa+30pOP.

The infrared absorption spectrum of OP (Figure 1a) was similar to that of Aa (Figure 1b), except, mainly, for the

https://doi.org/10.1021/acssuschemeng.3c02992
ACS Sustainable Chem. Eng. XXXX, XXX, XXX−XXX

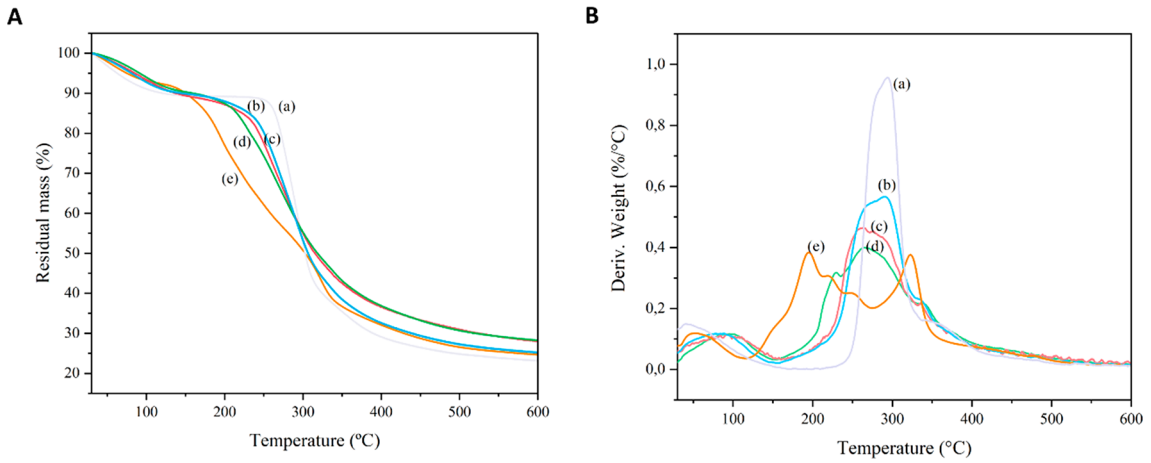

Figure 2. Thermogravimetric analysis. (A) TGA and (B) DTGA of (a) Aa, (b) Aa + 30 pOP, (c) Aa + 30 sOP, (d) Aa + 30 hOP, and (e) OP.

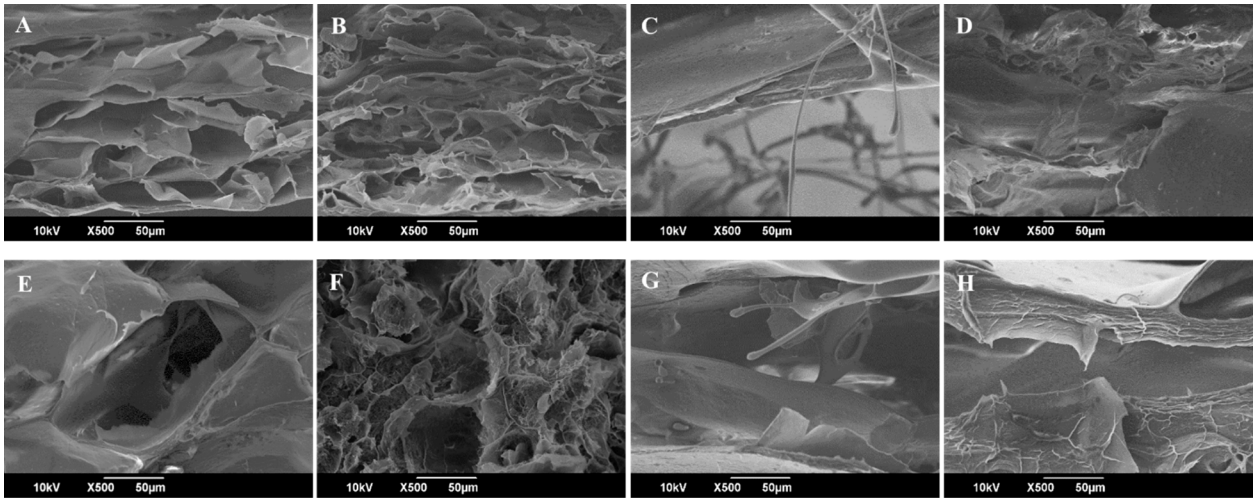

Figure 3. SEM micrographs of A: Aa, B: Aa+30 pOP, C: Aa+30 hOP, D: Aa+30 sOP, E: Aa+LMN, F: Aa+30pOP+LMN, G: Aa+30hOP+LMN, and H: Aa+30sOP+LMN. SEM micrographs were acquired at 500× and the scale bar = 50 μm.

presence of the C═O stretching band of the methoxyl ester groups ($COOCH_3$) at 1736 cm^{-1}. In the hydrogels with hOP, sOP, and hOP this band is still observable, but a new band centered at 1708 cm^{-1} appears, associated with the C═O stretching bands of the free carboxyl groups (COOH). This peak was particularly observed in the materials obtained with hOP since during the hydrolysis process (pH ≈ 3.5) the demethoxylation of pectin occurs.[38] Besides, the intensity of the stretching vibration band of hydroxyl groups (O−H) in Aa with a maximum intensity at 3358 cm^{-1}, increased significantly after the addition of OP in its different ways. This increase was significantly higher after the addition of hOP, suggesting that new hydrogen bonds were formed, in particular in the hydrogels prepared from the combination of Aa and hOP. The other bands that appear at 1013, 1145, and 1050 cm^{-1} in OP indicate the presence and predominance of typical pectin homogalacturonan structures and were also mainly observed in the materials prepared with hOP, which suggests that the hydrolytic treatment was the one releasing more pectin polymer from the vegetable cell wall among all the treatments done.[39] Similar results were observed for the FTIR of the materials containing LMN (Figure S2).

The same samples analyzed by FTIR were also analyzed by TGA (Figure 2) to elucidate changes in hydrogel constituents' thermal degradation temperatures and, consequently, potential interactions among them. As shown in Figure 2A,B (a), Aa presented a two-stage thermal degradation profile. The first one, associated with the evaporation of water molecules, showed a temperature of the maximum rate of weight loss (T_{max}) at approximately 50 °C and represented a mass loss of 10.8% (Figure 2A (a)). The second stage, which ranged from 200 to 600 °C, with a T_{max} = 294.8 °C, is attributed to the degradation of the polysaccharide.[40] In the case of OP (Figure 2A,B (b)), a much more complex thermal degradation profile was observed, given the presence of various polymers in the plant cell wall. The first degradation event that extends up to 115 °C is attributed to the presence of water molecules and other volatile compounds and represents a 7.5% weight loss (Figure 2A (b)). Then, in the second stage of thermal degradation, several overlapping peaks are observed, corresponding to pectin (T_{max} = 195 °C), hemicelluloses (T_{max} = 220 and 251 °C), and cellulose (T_{max} = 321 °C), according to what was previously reported in the literature.[41,42]

In the case of the Aa+OP hydrogels, their degradation profile results from a combination of the two components. In general, there is a first event that is attributed to the elimination of water molecules, in all cases taking place up to approximately 160 °C (Figure 2B (b−d)) and with an

https://doi.org/10.1021/acssuschemeng.3c02992
ACS Sustainable Chem. Eng. XXXX, XXX, XXX−XXX

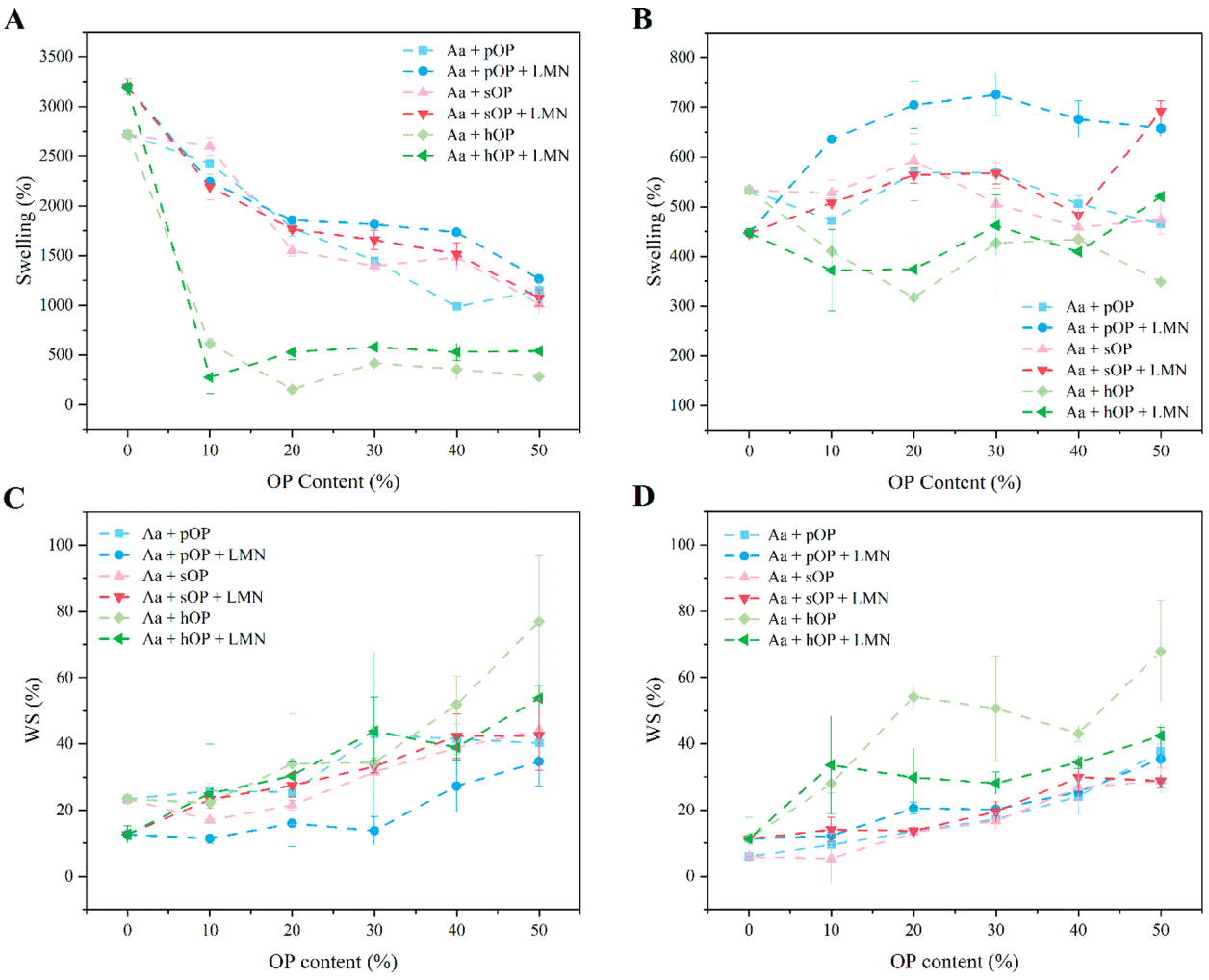

Figure 4. Swelling percentage of Aa + OP hydrogels with or without LMN as a function of OP content in A: Distilled water and B: Tap water and water solubility (WS) of Aa + OP hydrogels with or without LMN as a function of OP content in C: Distilled water and D: Tap water.

associated mass loss of 10% (Figure 2A (b–d)). The T_{max} of this first event, in all cases, was about 30 °C higher than that of the individual components, Aa and OP. This result suggests that water molecules are held strongly by the Aa+OP hydrogels when compared with Aa alone since more energy is needed to evaporate the water molecules. The second, more complex event represents the degradation of the polymers present in OP together with Aa which is in a higher proportion. From Figure 2B it can be observed that the temperature of the maximum degradation rate, corresponding to Aa, shifts from 295 to 291 °C for Aa + 30% pOP, whereas it moves to 264 °C for both Aa + 30% sOP and Aa + 30% hOP, showing that Aa has a stronger interaction with pOP, in agreement with FTIR results. Particularly in Aa + 30% hOP, the broad peak with T_{max} = 264 °C shows two shoulders, one at 230 °C and the other at 340 °C. These two shoulders are attributed to the presence of polymers such as pectin, hemicelluloses, and cellulose that have been released from the OP vegetable cell wall to the solution media during the process of hydrolysis.[42] Similar results were observed for the hydrogels prepared with LMN (Figure S3). According to its datasheet, raw LMN has a boiling point at 175.5 °C; still, in Figure S3Ba its evaporation is associated with the sharp peak appearing at 210 °C for the Aa+LMN hydrogel. This shift to higher temperatures suggests a strong interaction of LMN with agar molecules. Nevertheless, since the content of LMN present in the hydrogels (1.5 wt %) was low and LMN evaporation is overlapped with OP degradation, it was difficult to observe this peak in the thermal curves of Aa+OP+LMN hydrogels.

Finally, a morphological analysis of the swelled hydrogels was done by observing their microstructure after freeze-drying. Figure 3 shows the SEM micrographs for Aa, Aa+LMN, and their hydrogels with 30 wt % pOP, sOP, or hOP. Very clear morphological differences were observed between Aa (Figure 3A) and Aa+LMN (Figure 3E). The Aa cross-section surface indicated highly porous samples with 50–70 μm average pores sizes, while Aa+LMN hydrogels also showed high porosity but with bigger and better defined cavity-like structures, of about 100–170 μm. After the addition of the unprocessed OP powder, pOP, the hydrogels maintained their highly porous structure, but their pore size decreased significantly compared to Aa and Aa+LMN hydrogels. On the contrary, after adding hOP (Figure 3C,G) or sOP (Figure 3D,H), the porosity was mostly lost, and only very few small pores could be identified. Interestingly, when hOP was added to Aa the presence of filamentous structures was observed at the micro- and macroscopic level (after the freeze-drying process of the gel previously swelled in tap water during 24 h). Most likely, the hydrolysis method released pectin and hemicelluloses, which formed filamentary structures, which were observed as a

https://doi.org/10.1021/acssuschemeng.3c02992
ACS Sustainable Chem. Eng. XXXX, XXX, XXX−XXX

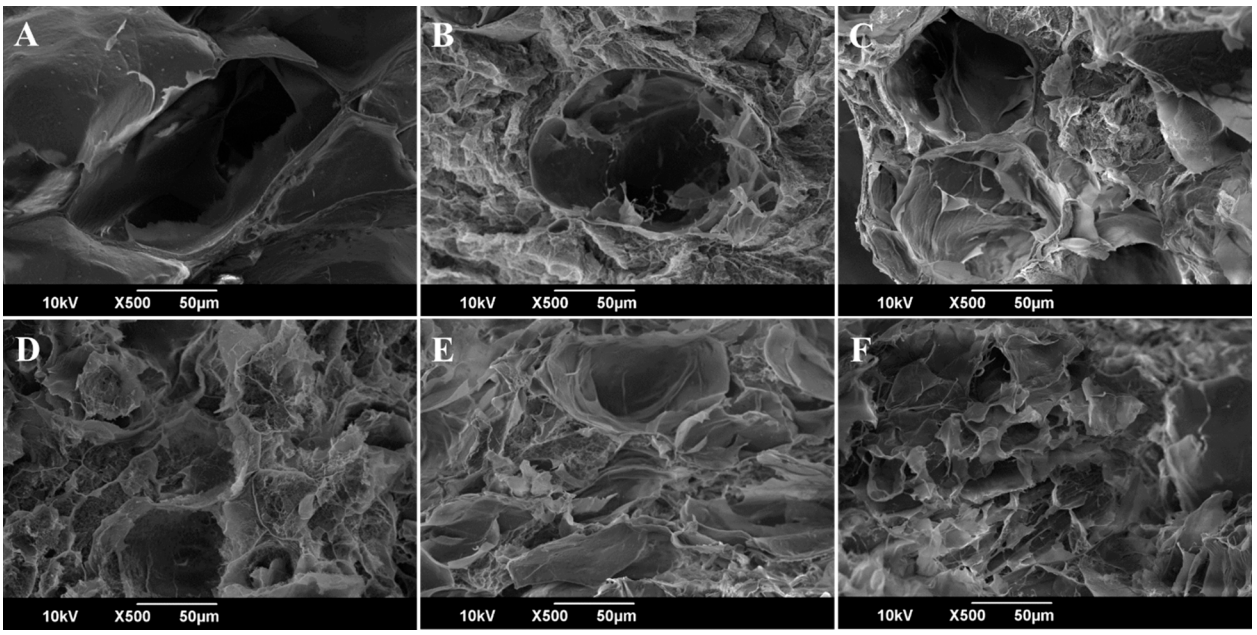

Figure 5. SEM micrographs of A: Aa+LMN, B: Aa+10pOP+LMN, C: Aa+20pOP+LMN, D: Aa+30pOP+LMN, E: Aa+40pOP+LMN, and F: Aa +50pOP+LMN.

second phase. For the materials obtained by treating OP with ultrasound, it was observed that the surface of the gels was smooth with very few available pores. In some micrographs, however, the presence of filaments attributed to the components present in OP interacting with the surface of Aa were observed.

Swelling and Solubility of Hydrogels in Distilled and Tap Water. Aa hydrogels consist of polymer molecules linked by hydrogen bonds that form a network or macroreticule with the capacity to store large amounts of water molecules.[7] These hydrogels showed a swelling capacity of 2720.0% ± 7.9% in distilled water (Figure 4A, 0% OP content) and 533.3% ± 7.6% in tap water (Figure 4B, 0% OP content).

The reduced capability of Aa hydrogels to absorb tap water with respect to distilled water is well reported. Distilled water is free of ions and impurities, while tap water contains ions of salts, minerals, or other dissolved substances. When the ionic Aa hydrogel is in the aqueous saline medium (tap water), two phenomena can occur, seriously compromising its swelling capacity. The first one is that di- or trivalent cations can form new cross-linking points that reduce the hydrogels' expansion capability. The second one is that tap water ions can interact with the negatively charged groups on the polysaccharide chains of Aa, causing them to become less effective at absorbing water.[43,44]

The presence of ions in the aqueous absorption media also affected the solubility of the Aa hydrogels. For instance, the Aa solubility changed from 23.3% ± 1.3% in distilled water to 5.9% ± 0.1% in tap water (Figure 4C,D, 0% OP). This observation suggests that the interaction of the ions in the tap water with low molecular weight charged species in Aa (i.e., agaropectin, the nongelling component of agar) stabilizes them and prevents them from dissolving, as in distilled water. Indeed, the polar nature of such species increases their ability to interact with water molecules through electrostatic interactions in the distilled water and thus to be dissolved.

The incorporation of LMN in Aa (0% OP) affected the swelling capacity of the hydrogels. As observed in Figure 4A, in distilled water, it increased the hydrogels' absorption capacity, whereas in tap water, it slightly decreased it (Figure 4B). At the same time, the addition of LMN into Aa (0% OP) caused a decrease in the hydrogels' water solubility in distilled water (Figure 4C), while in tap water the differences were within the experimental error (Figure 4D). Evidently, the LMN increased the density of negative charges in the hydrogel (Z-potential = −30 mV), increasing the polarity and thus the interaction with water molecules, producing these results. In the presence of the tap water ions this effect is much reduced due to their interactions with the polymer's charged chains. Similar observations were previously reported in the literature for agar hydrogels and plant extracts. For example, Atef et al.[45] reported an increase in the swelling percentage of agar/cellulose nanocomposites with savory essential oil, and Kanmani et al.[46] found that agar films with grapefruit seed extract had a higher moisture content than control agar films.

Concerning the effect of the addition of OP to the hydrogel formulation, it was observed that for the swelling in distilled water increments in the content of OP produced a decrease in the swelling capacity of the Aa hydrogels (Figure 4A). The reduction in the swelling capacity of Aa+OP and Aa+OP +LMN hydrogels could be mainly caused by the physical interactions between Aa and the polymers present in OP that prevent agar supramolecular structure formation, limiting their swelling capacity. This decrease was particularly significant in the case of the materials prepared with hOP, in which we have demonstrated by FTIR and TGA that the hydrolysis mainly released pectin polymer and led to the formation of filamentous structures with the absence of porosity, according to SEM observations. The difference in the swelling capacity of the hydrogels with hOP was also accompanied by a higher solubility in distilled and tap water, reaching 76.8 ± 18.9% (Figure 4C) and 67.9% ± 15.3% (Figure 4D), respectively.

Regarding the performance of the hydrogels in tap water, it was generally observed that the combination of OP with LMN in the gels produced an increase in their swelling capacity compared to those that only had OP, regardless of its previous

https://doi.org/10.1021/acssuschemeng.3c02992
ACS Sustainable Chem. Eng. XXXX, XXX, XXX−XXX

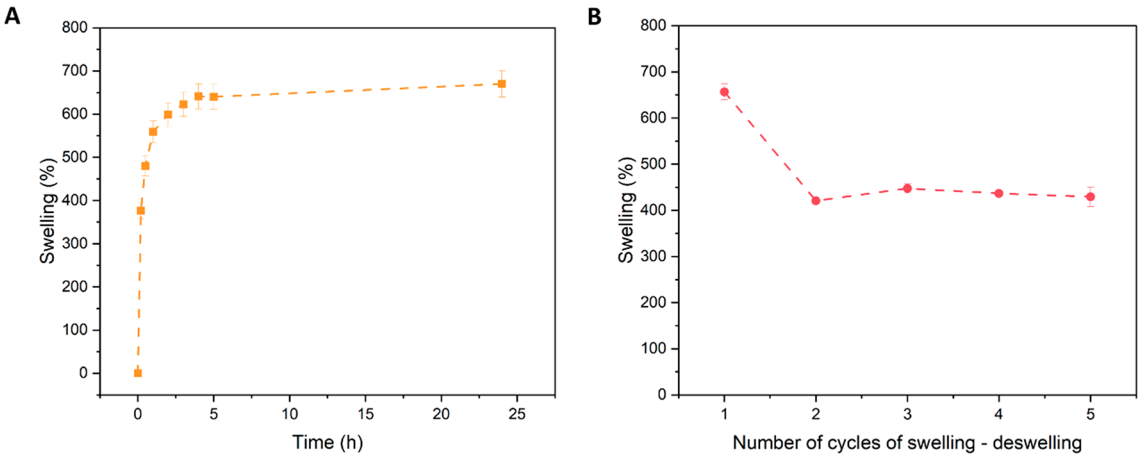

Figure 6. Swelling of Aa+50pOP+LMN in tap water (%) as a function of A: Immersion time for the first swelling and B: Maximum swelling in tap water (%) after 24 h, as a function of the number of swelling−deswelling cycles.

treatment (Figure 4B). However, when this last factor is taken into account, a strong impact on the swelling capacity of the hydrogels is observed. Those prepared with hOP had the lowest performance, those prepared by sonication showed a slight increase in swelling, and the ones prepared with pOP had the highest swelling, exceeding 700%.

Although the addition of different percentages of OP did not induce significant differences in the swelling capacity of the hydrogels in tap water, it affected their solubility, which increased almost linearly with the increase in the OP content (Figure 4D). The hydrogels showing the highest solubility in tap water were the ones that incorporated hOP, possibly due to the presence of species of lower molecular weight that after, the hydrolysis of OP, have been able to dissolve easily in water. The percentage of solubility in tap water for Aa+hOP+LMN increased from approximately 11% to 43%, for 0 to 50 wt % hOP, respectively. For the samples Aa+sOP+LMN and Aa +pOP+LMN, the WS increased from 11% to 28% and 35%, respectively, for 0 to 50% OP, which is why higher percentages of OP were not considered. The solubility reported here is lower with respect to that presented by Kanmani et al.,[46] who reported an increase in the solubility of agar films from 10% to 61% with the addition of grapefruit seed extract, and by Giménez et al.,[47] who reported that the addition of green tea extract to agar films produced an increase in its solubility from 24% to 58%, at a fixed amount of plasticizer in each case.

Considering that the Aa+pOP+LMN hydrogels showed the best swelling capacity, their micromorphologies for different pOP concentrations are reported in Figure 5. The SEM images clearly demonstrate porous structures with interconnected micropores for all of them, and a decrease in the pores' size with the increase in pOP concentration.

Based on the previous results and considering that a high content of vegetable waste is of significant importance for increasing the fertilizer properties of the hydrogels, reducing their price, and contributing to the circular economy, the Aa +50pOP+LMN hydrogel was selected as the best candidate to evaluate its performance as an active soil conditioner. Therefore, the curve of swelling in tap water vs time and the effect of five swelling−deswelling cycles on the swelling capability of Aa+50pOP+LMN hydrogels were evaluated. Results included in Figure 6 show that the swelling capacity of Aa+50pOP+LMN can reach approximately 400% in only 10 min and more than 500% in 1 h, equilibrating at about 700% after about 4 h. This rapid swelling can be explained by the porous structure observed in SEM (Figure 5F), which provides efficient channels for fast water transport. Besides, in Figure 6 it can be seen that Aa+50pOP+LMN experienced superior swelling in the first cycle. Then, at the subsequent cycles, its swelling capacity decreased but remained constant around 430%. This phenomenon could be associated with the effect of cross-linking of pectin molecules by divalent cations present in the tap water, but it can also be related to the solubility of low molecular weight charged species that produced a decrease in the hydrogel swelling.[43,44]

Biopesticide Properties. The antimicrobial activity of Aa +50pOP+LMN was investigated against phytopathogens *Psy* and *F. eumartii*. For the antibacterial test, grown *Psy* cell suspension cultures were incubated with different concentrations of hydrogels for 24 h, after which the optical density at 600 nm (OD_{600}) of the solutions was used to evaluate the bacterial growth. The results (Figure S5) show that Aa+50pOP +LMN did not affect *Psy* growth. Similarly, in an attempt to assess Aa+50pOP+LMN antifungal properties, *F. eumartii* spores were incubated with different concentrations of the hydrogel for 24 h. However, the results (Figure S6) showed that none of the concentrations tested inhibited the germination of the spores of *F. eumartii*, suggesting that hydrogels do not have antifungal activity under the tested conditions. Since several reports are showing that limonene possesses antimicrobial activity,[17,18,48,49] our findings suggest that the presence of LMN in Aa+50pOP+LMN may not be sufficient to induce an antimicrobial effect. Alternatively, the absence of an antibiotic effect could be attributed to the molecule's strong binding or interaction with the hydrogel matrix, as evidenced by TGA analysis (Figure S3Ba). Furthermore, in the literature, the antibacterial activity of LMN is usually enhanced by its combination with other compounds such as the ones naturally occurring in essential oils or other common antimicrobials such as nisin peptide or ε-polylysine.[50−52]

Effect of the Soil Conditioner Aa+50pOP+LMN on Tomato Plants Subjected to Water Stress. The ability of the Aa+50pOP+LMN hydrogel to retain moisture in the soil was monitored during a mild drought simulation experiment. Tomato plants were grown in pots supplemented with a commercial substrate for 18 days under irrigation conditions, and then 0.5% by weight or 2.5% by weight of Aa+50pOP

https://doi.org/10.1021/acssuschemeng.3c02992
ACS Sustainable Chem. Eng. XXXX, XXX, XXX−XXX

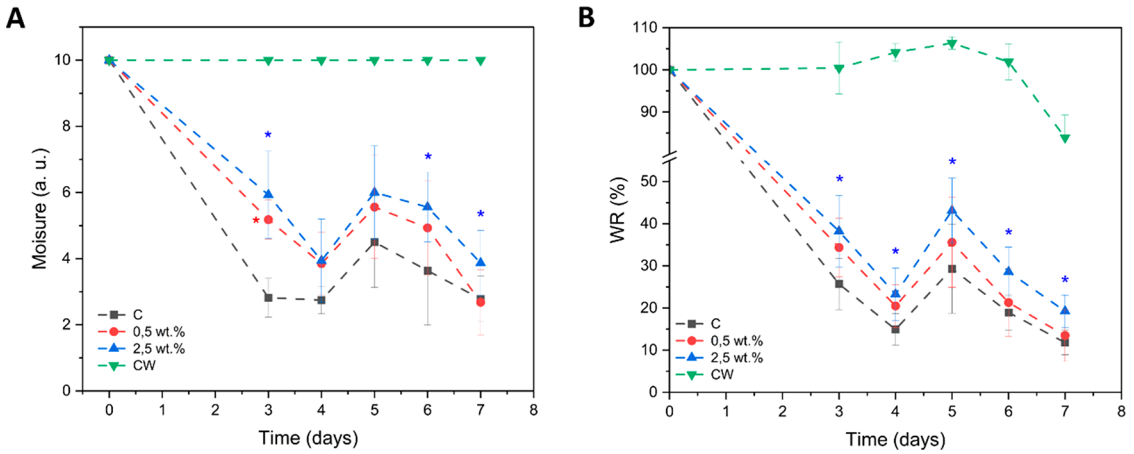

Figure 7. Moisture and water retention ability of each substrate after stopping the water supply. Moisture (A) and water retention (B) without hydrogel supplementation (C) or containing hydrogel 0.5 or 2.5 wt % are indicated. As irrigation control, the substrate without hydrogel was continually watered along the experiment (CW). On day 4 of water stress, plants were rewatered with the volume of water necessary to reach 50% field capacity of the C plants. Water retention was measured by weighting pots every day and 100% represents the weights of pots at field capacity. Values are the mean (±SD) of one experiment using 8 plants per treatment. The data from each of the days were subjected to analysis of variance (ANOVA) with Dunnett's test, and the * indicates a significant difference ($p < 0.05$) of each treatment with respect to the control plants without conditioner supplement on each day.

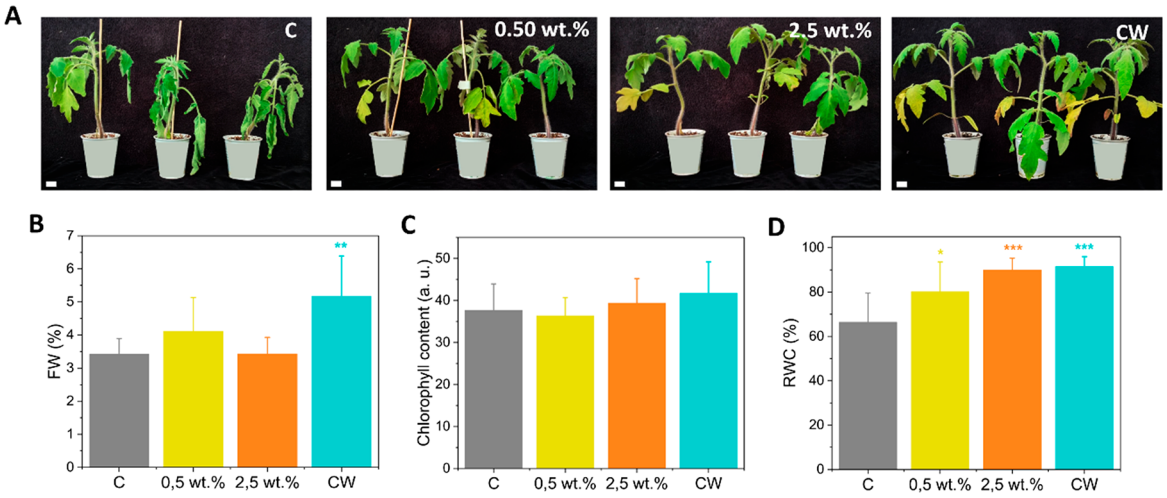

Figure 8. Effect of hydrogel substrate supplementation on tomato plants subjected to drought for 7 days. A: Representative plants of each treatment are shown. Bar = 1 cm. B: Quantification of the aerial biomass (FW) after 7 days of suspending irrigation (28-day-old seedlings). C: Chlorophyll content. D: Relative water content (RWC) of the leaves of the tomato plant at the end of the experiment. Values are the mean (±SD) of one experiment using 8 plants per treatment. The data were subjected to analysis of variance (ANOVA) with Dunnett's test, and the asterisks indicate a significant difference (*$p < 0.05$; **$p < 0.01$; ***$p \leq 0.005$) of each treatment with respect to the control plants without conditioner supplement.

+LMN was added and irrigated at field capacity for the next 3 days. Following that, irrigation was discontinued and reintroduced just once after 4 days of drought but only to reach 50% of the C plants' field capacity.

As shown in Figure 7A, while soil moisture decreased drastically in control C without the hydrogel, the presence of the hydrogel helped to maintain soil moisture at higher levels throughout the experiment. The moisture content of the soil that received continuous irrigation (CW) is also shown in Figure 7A as a reference for a fully moist soil. After 3 days of drought, the moisture content of substrate C decreased by approximately 70% when compared to CW, while the moisture content of substrates supplemented with conditioner decreased less, allowing for nearly 20% and 30% more water savings for substrates containing 0.5 and 2.5 wt % hydrogel conditioners, respectively. At the end of the drought test (day 7), substrates supplemented with 2.5 wt % conditioner retained 10% more moisture than the C.

On the other hand, in Figure 7B it can be seen the water retention capacity of the substrates supplemented with 0.5 and 2.5 wt % of the developed hydrogels. From the third day of drought, the water retention was higher in the substrates supplemented with 2.5 wt % hydrogels than in the substrates supplemented with 0.5 wt %. On the seventh day of water stress, the substrates supplemented with 2.5 wt % of hydrogel showed a 12% higher water retention capacity than the control C, and nonsignificant differences were found in the substrates supplemented with 0.5 wt % of hydrogel. Therefore, these results indicate that the functional capacity of the substrate is critically dependent on the amount of conditioner added.

https://doi.org/10.1021/acssuschemeng.3c02992
ACS Sustainable Chem. Eng. XXXX, XXX, XXX−XXX

Furthermore, the effect of the supplementation of the substrate with the soil conditioner hydrogel on the growth parameters of 28-day-old tomato plants subjected to drought for 7 days was studied (Figure 8A,B). As expected, tomato plants grown in the absence of a conditioner but continuously watered (CW) and without daily irrigation (C) were different (Figure 8A). C plants grown in nonsupplemented substrate and subjected to drought stress were approximately 30% smaller than CW plants (Figure 8B). Plants grown in 0.5 wt % hydrogel-supplemented substrate had a 20% increase in the fresh weight (FW) compared to C (Figure 8B), and similar results were observed for the dry weight (Figure S7). However, a substrate supplementation of 2.5 wt % was unsuitable for improving plant biomass over C. This result could be attributed to the LMN concentration in the soil, which may have exceeded the limit that causes toxic effects in plants, counterbalancing the positive effect of water retention and preventing an increase in the plants aerial biomass (Figure S8).[53] However, no significant differences in the plant chlorophyll content were observed across all treatments (Figure 8C). Finally, the relative water content (RWC) in the leaves of the control tomato plants (C) was affected by drought stress and reached approximately 60% RWC (Figure 8D). Plants grown in substrates supplemented with 0.5 wt % and 2.5 wt % conditioner, on the other hand, maintained RWC values comparable to the continuously irrigated control (CW), indicating no reduction in water availability for plants.

In-Soil Biodegradability of the Aa+50pOP+LMN Soil Conditioner. Lastly, a three month experiment was conducted to assess the Aa+50pOP+LMN hydrogel's biodegradability in a commercial soil. At days 5, 15, 30, and 60, samples were unburied, and their weight was determined by using an analytical balance after meticulous cleaning and drying. As seen in Figure 9, Aa+50pOP+LMN initially degraded quickly, losing about 45% of their weight after only 15 days, and then degraded slowly and steadily, losing 52% of their weight after three months. The hydrogels' color also changed, going from a bright yellow to a light brown, possibly as a result of the OP's typical orange pigments degradation.

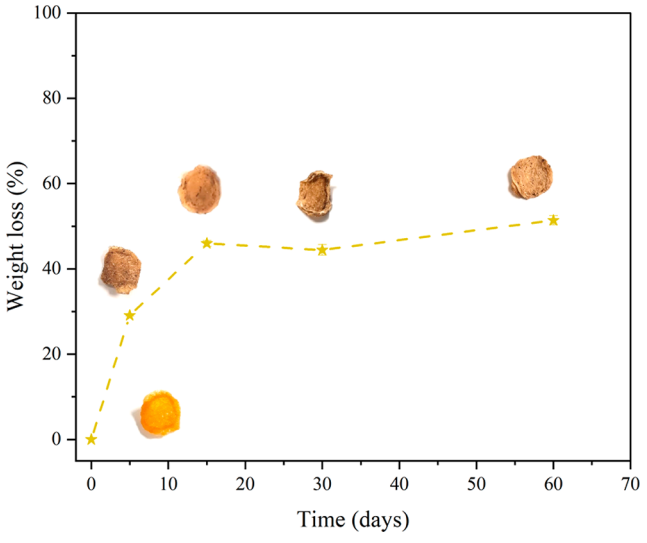

Figure 9. Biodegradability of the Aa+50pOP+LMN hydrogel in commercial soil. Weight loss (%) vs time (days). Photographs of the hydrogels during the experiment are included next to each data point.

However, the hydrogels kept their structure and function, as evidenced by the aspect of the unburied samples, suggesting that this material could offer good time frame stability for the proposed application.

CONCLUSIONS

A fully biobased soil conditioner based on agar polymer was prepared, and its swelling capacity was optimized by the addition of 50 wt % orange peel powder and 1.5 wt % limonene nanoemulsion. The different ingredients showed good compatibility, as demonstrated by FTIR, TGA, and SEM, and produced hydrogels with an increased number of smaller pores compared to agar hydrogels alone. In addition, the soil conditioner showed rapid swelling in tap water, reaching 400% in only 10 min and reaching an equilibrium swelling of 430% after five cycles of swelling−deswelling in tap water. Furthermore, this hydrogel has an appropriate biodegradability rate in soil, reaching a 52% weight loss after 3 months of experiment. However, unexpectedly, the presence of LMN in the hydrogel did not show antibacterial or antifungal activity when tested against two widely known phytopathogens: the bacterium *Pseudomonas syringe* and the fungus *Fusarium solani*. Finally, the addition of 2.5 wt % hydrogel to the soil led to a 10% increase in water retention after 7 days of simulated drought conditions compared to the control without hydrogel, and both hydrogel percentages enhanced the relative water content of tomato leaves.

ASSOCIATED CONTENT

Supporting Information

The Supporting Information is available free of charge at https://pubs.acs.org/doi/10.1021/acssuschemeng.3c02992.

FTIR, TGA, SEM, biopesticide properties, dry weight of tomato plants grown under drought stress, and cytotoxicity test of soil conditioners (PDF)

AUTHOR INFORMATION

Corresponding Authors

Danila Merino − *Smart Materials, Istituto Italiano di Tecnologia, Genova 16163, Italy;* orcid.org/0000-0002-5098-8550; Phone: +39 010 28961; Email: danila.merino@ehu.eus

Athanassia Athanassiou − *Smart Materials, Istituto Italiano di Tecnologia, Genova 16163, Italy;* orcid.org/0000-0002-6533-3231; Email: athanassia.athanassiou@iit.it

Authors

Andrea Yamila Mansilla − *Instituto de Investigaciones Biológicas (IIB), UE CONICET-UNMDP, Facultad de Ciencias Exactas y Naturales, Universidad Nacional de Mar del Plata (UNMDP) y Consejo Nacional de Investigaciones Científicas y Técnicas (CONICET), 7600 Mar del Plata, Argentina*

María Florencia Salcedo − *Instituto de Investigaciones Biológicas (IIB), UE CONICET-UNMDP, Facultad de Ciencias Exactas y Naturales, Universidad Nacional de Mar del Plata (UNMDP) y Consejo Nacional de Investigaciones Científicas y Técnicas (CONICET), 7600 Mar del Plata, Argentina*

Complete contact information is available at: https://pubs.acs.org/10.1021/acssuschemeng.3c02992

https://doi.org/10.1021/acssuschemeng.3c02992
ACS Sustainable Chem. Eng. XXXX, XXX, XXX−XXX

Notes

The authors declare no competing financial interest.

■ ACKNOWLEDGMENTS

The authors would like to thank Lara Marin for acquiring the TGA curves and to IIT for their initiative on sustainability issues.

■ REFERENCES

(1) Food and Agriculture Organization of the United Nations (FAO). *Transforming Food and Agriculture to Achieve the SDGs*, 2018.
(2) The Intergovernmental Panel on Climate Change (IPCC). *Climate Change and Land: An IPCC Special Report on Climate Change, Desertification, Land Degradation, Sustainable Land Management, Food Security, and Greenhouse Gas Fluxes in Terrestrial Ecosystems*, 2019.
(3) Food and Agriculture Organization of the United Nations, (FAO). *SDG no. 2: End Hunger, Achieve Food Security and Improved Nutrition and Promote Sustainable Agriculture.*
(4) de Vasconcelos, M. C.; Gomes, R. F.; Sousa, A. A. L.; Moreira, F. J. C.; Rodrigues, F. H. A.; Fajardo, A. R.; Neto, L. G. P. Superabsorbent Hydrogel Composite Based on Starch/Rice Husk Ash as a Soil Conditioner in Melon (Cucumis Melo L.) Seedling Culture. *Journal of Polymers and the Environment* **2020**, *28* (1), 131−140.
(5) Guilherme, M. R.; Aouada, F. A.; Fajardo, A. R.; Martins, A. F.; Paulino, A. T.; Davi, M. F. T.; Rubira, A. F.; Muniz, E. C. Superabsorbent Hydrogels Based on Polysaccharides for Application in Agriculture as Soil Conditioner and Nutrient Carrier: A Review. *Eur. Polym. J.* **2015**, *72*, 365−385.
(6) Rizwan, M.; Rubina Gilani, S.; Iqbal Durani, A.; Naseem, S. Materials Diversity of Hydrogel: Synthesis, Polymerization Process and Soil Conditioning Properties in Agricultural Field. *Journal of Advanced Research* **2021**, *33*, 15−40.
(7) Lyons, J. G.; Geever, L. M.; Nugent, M. J. D.; Kennedy, J. E.; Higginbotham, C. L. Development and Characterisation of an Agar-Polyvinyl Alcohol Blend Hydrogel. *Journal of the Mechanical Behavior of Biomedical Materials* **2009**, *2* (5), 485−493.
(8) Merino, D.; Alvarez, V. A. Advanced Applications of Green Materials in Agriculture 8. In *Applications of Advanced Green Materials*; Elsevier Ltd., 2021; pp 193−222. DOI: 10.1016/B978-0-12-820484-9.00008-8.
(9) Abobatta, W. Impact of Hydrogel Polymer in Agricultural Sector. *Advances in Agriculture and Environmental Science* **2018**, *1*, 59−64.
(10) Ejaz, M. K.; Aurangzaib, M.; Iqbal, R.; Shahzaman, M.; Habib-Ur-rahman, M.; El-Sharnouby, M.; Datta, R.; Alzuaibr, F. M.; Sakran, M. I.; Ogbaga, C. C.; Sabagh, A. El. The Use of Soil Conditioners to Ensure a Sustainable Wheat Yield under Water Deficit Conditions by Enhancing the Physiological and Antioxidant Potentials. (Land (2022), 11, 368). *Land* **2022**, *11*, 368.
(11) Sharma, K.; Kumar, V.; Swart-Pistor, C.; Chaudhary, B.; Swart, H. C. Synthesis, Characterization, and Anti-Microbial Activity of Superabsorbents Based on Agar-Poly(Methacrylic Acid-Glycine). *J. Bioact. Compat. Polym.* **2017**, *32* (1), 74−91.
(12) Chaudhary, J.; Thakur, S.; Sharma, M.; Gupta, V. K.; Thakur, V. K. Development of Biodegradable Agar-Agar/Gelatin-Based Superabsorbent Hydrogel as an Efficient Moisture-Retaining Agent. *Biomolecules* **2020**, *10* (6), 939.
(13) Singh, J.; Singh, B.; Vishavnath. Designing Starch-Alginate Hydrogels for Controlled Delivery of Fungicide for the Alleviation of Environmental Pollution. *ACS Agricultural Science and Technology* **2022**, *2*, 1239.
(14) United Nations. *SDG 12: Ensure Sustainable Consumption and Production Patterns.*
(15) Quilez-Molina, A. I.; Merino, D. From Waste to Resource: Methods for Vegetable Waste Transformation into Sustainable Plant-Based Bioplastics. *Advanced Applications of Biobased Materials* **2023**, 61−110.
(16) de Andrade Rodrigues, R. M. B.; da Silva Fontes, L.; de Carvalho Brito, R.; Barbosa, D. R. e. S.; das Graças Lopes Citó, A. M.; do Carmo, I. S.; de Jesus Sousa, E. M.; Silva, G. N. A Sustainable Approach in the Management of Callosobruchus Maculatus: Essential Oil of Protium Heptaphyllum and Its Major Compound d-Limonene as Biopesticides. *Journal of Plant Diseases and Protection* **2022**, *129* (4), 831−841.
(17) Rancic, A.; Sokovic, M.; Van Griensven, L.; Vukojevic, J.; Brkic, D.; Ristic, M. Antimicrobial Activity of Limonene. *Zbornik radova* **2003**.
(18) Feng, J.; Wang, R.; Chen, Z.; Zhang, S.; Yuan, S.; Cao, H.; Jafari, S. M.; Yang, W. Formulation Optimization of D-Limonene-Loaded Nanoemulsions as a Natural and Efficient Biopesticide. *Colloids Surf., A* **2020**, *596* (January), No. 124746.
(19) Ibrahim, M.A.; Kainulainen, P.; Aflatuni, A. Insecticidal, Repellent, Antimicrobial Activity and Phytotoxicity of Essential Oils: With Special Reference to Limonene and Its Suitability for Control of Insect Pests. *Agricultural and Food Science in Finland* **2001**, *10* (3), 243−259.
(20) Abdul Khalil, H. P. S.; Lai, T. K.; Tye, Y. Y.; Rizal, S.; Chong, E. W. N.; Yap, S. W.; Hamzah, A. A.; Nurul Fazita, M. R.; Paridah, M. T. A Review of Extractions of Seaweed Hydrocolloids: Properties and Applications. *Express Polymer Letters* **2018**, *12* (4), 296−317.
(21) Armisén, R.; Galatas, F. Agar. In *Handbook of Hydrocolloids*, Second ed.; Woodhead Publishing Series in Food Science, Technology and Nutrition; Woodhead Publishing, 2009, pp 82−107. DOI: 10.1533/9781845695873.82.
(22) European Food Safety Authority. Scientific Opinion: Re-Evaluation of Agar (E 406) as a Food Additive. *EFSA Journal* **2016**, *14*, (12) 4645, http://doi.wiley.com/10.2903/j.efsa.2016.4645
(23) Suri, S.; Singh, A.; Nema, P. K. Current Applications of Citrus Fruit Processing Waste: A Scientific Outlook. *Applied Food Research* **2022**, *2* (1), No. 100050.
(24) Food and Agriculture Organization of the United Nations. *FAOSTAT*.
(25) Merino, D.; Bellassi, P.; Paul, U. C.; Morelli, L.; Athanassiou, A. Assessment of Chitosan/Pectin-Rich Vegetable Waste Composites for the Active Packaging of Dry Foods. *Food Hydrocolloids* **2023**, *139*, No. 108580.
(26) Fidalgo, A.; Ciriminna, R.; Carnaroglio, D.; Tamburino, A.; Cravotto, G.; Grillo, G.; Ilharco, L. M.; Pagliaro, M. Eco-Friendly Extraction of Pectin and Essential Oils from Orange and Lemon Peels. *ACS Sustainable Chem. Eng.* **2016**, *4* (4), 2243−2251.
(27) Ibrahim, M. A.; Oksanen, E. J.; Holopainen, J. K. Effects of Limonene on the Growth and Physiology of Cabbage (Brassica Oleracea L) and Carrot (Daucus Carota L) Plants. *Journal of the Science of Food and Agriculture* **2004**, *84* (11), 1319−1326.
(28) Ansari, I. A.; Akhtar, M. S. Current Insights on the Role of Terpenoids as Anticancer Agents: A Perspective on Cancer Prevention and Treatment. In *Natural Bio-active Compounds*; Swamy, M., Akhtar, M., Eds.; Springer, Singapore, 2019; pp 53−80. DOI: 10.1007/978-981-13-7205-6_3.
(29) King, E. O.; Ward, M. K.; Raney, D. E. Two Simple Media for the Demonstration of Pyocyanin and Fluorescin. *Journal of laboratory and clinical medicine* **1954**, *44* (2), 301−307.
(30) Mansilla, A. Y.; Albertengo, L.; Rodríguez, M. S.; Debbaudt, A.; Zúñiga, A.; Casalongué, C. A. Evidence on Antimicrobial Properties and Mode of Action of a Chitosan Obtained from Crustacean Exoskeletons on Pseudomonas Syringae Pv. Tomato DC3000. *Appl. Microbiol. Biotechnol.* **2013**, *97* (15), 6957−6966.
(31) de Castro e Silva, P.; de Oliveira, A. C. S.; Pereira, L. A. S.; Valquiria, M.; Carvalho, G. R.; Miranda, K. W. E.; Marconcini, J. M.; Oliveira, J. E. Development of Bionanocomposites of Pectin and Nanoemulsions of Carnauba Wax and Neem Oil Pectin/Carnauba Wax/Neem Oil Composites. *Polym. Compos.* **2020**, *41* (3), 858−870.
(32) Cofelice; Cuomo; Chiralt. Alginate Films Encapsulating Lemongrass Essential Oil as Affected by Spray Calcium Application. *Colloids and Interfaces* **2019**, *3* (3), 58.

https://doi.org/10.1021/acssuschemeng.3c02992
ACS Sustainable Chem. Eng. XXXX, XXX, XXX−XXX

(33) Mendieta, J. R.; Pagano, M. R.; Muñoz, F. F.; Daleo, G. R.; Guevara, M. G. Antimicrobial Activity of Potato Aspartic Proteases (StAPs) Involves Membrane Permeabilization. *Microbiology* **2006**, *152* (7), 2039−2047.
(34) Jamnongkan, T.; Kaewpirom, S. Potassium Release Kinetics and Water Retention of Controlled-Release Fertilizers Based on Chitosan Hydrogels. *Journal of Polymer and the Environment* **2010**, *18*, 413−421.
(35) Patanè, C.; Scordia, D.; Testa, G.; Cosentino, S. L. Physiological Screening for Drought Tolerance in Mediterranean Long-Storage Tomato. *Plant Science* **2016**, *249*, 25−34.
(36) Merino, D.; Alvarez, V. A. In-Soil Biodegradation Behavior Of Chitosan-Coated Phosphorylated Starch Films. *Advanced Materials Letters* **2019**, *10* (12), 907−912.
(37) Davidović, S.; Lazić, V.; Miljković, M.; Gordić, M.; Sekulić, M.; Marinović-Cincović, M.; Ratnayake, I. S.; Ahrenkiel, S. P.; Nedeljković, J. M. Antibacterial Ability of Immobilized Silver Nanoparticles in Agar-Agar Films Co-Doped with Magnesium Ions. *Carbohydr. Polym.* **2019**, *224* (June). DOI: 10.1016/j.carbpol.2019.115187.
(38) Thakur, S.; Chaudhary, J.; Kumar, V.; Thakur, V. K. Progress in Pectin Based Hydrogels for Water Purification: Trends and Challenges. *Journal of Environmental Management* **2019**, *238* (February), 210−223.
(39) Slavov, A.; Ognyanov, M.; Vasileva, I. Pectic Polysaccharides Extracted from Pot Marigold (Calendula Officinalis) Industrial Waste. *Food Hydrocolloids* **2020**, *101* (November 2019), No. 105545.
(40) Orsuwan, A.; Shankar, S.; Wang, L. F.; Sothornvit, R.; Rhim, J. W. Preparation of Antimicrobial Agar/Banana Powder Blend Films Reinforced with Silver Nanoparticles. *Food Hydrocolloids* **2016**, *60*, 476−485.
(41) Boumediene, M.; Benaïssa, H.; George, B.; Molina, S.; Merlin, A. Characterization of Two Cellulosic Waste Materials (Orange and Almond Peels) and Their Use for the Removal of Methylene Blue from Aqueous Solutions. *Maderas: Ciencia y Tecnologia* **2015**, *17* (1), 69−84.
(42) Merino, D.; Athanassiou, A. Alkaline Hydrolysis of Biomass as an Alternative Green Method for Bioplastics Preparation: In Situ Cellulose Nanofibrillation. *Chemical Engineering Journal* **2023**, *454*, No. 140171.
(43) Sultana, S.; Rahaman, S.; Hasnine, S. M. M. Hasnine Effect of Salinity on swelling behaviors of superwater absorbent hydrogel prepared from carboxymethyl cellulose/acrylamide blends by gamma radiation *Am. J. Appl. Ind. Chem.*2018 *2* (2), 20−26,
(44) Flory, P. J. *Principles of Polymer Chemistry*; Cornell University Press, 1953.
(45) Atef, M.; Rezaei, M.; Behrooz, R. Characterization of Physical, Mechanical, and Antibacterial Properties of Agar-Cellulose Bionanocomposite Films Incorporated with Savory Essential Oil. *Food Hydrocolloids* **2015**, *45*, 150−157.
(46) Kanmani, P.; Rhim, J. W. Antimicrobial and Physical-Mechanical Properties of Agar-Based Films Incorporated with Grapefruit Seed Extract. *Carbohydr. Polym.* **2014**, *102* (1), 708−716.
(47) Giménez, B.; López de Lacey, A.; Pérez-Santín, E.; López-Caballero, M. E.; Montero, P. Release of Active Compounds from Agar and Agar-Gelatin Films with Green Tea Extract. *Food Hydrocolloids* **2013**, *30* (1), 264−271.
(48) Iacobellis, N. S.; Lo Cantore, P.; Capasso, F.; Senatore, F. Antibacterial Activity of Cuminum Cyminum L. and Carum Carvi L. Essential Oils. *J. Agric. Food Chem.* **2005**, *53* (1), 57−61.
(49) Abdel-Kawy, M. A.; Michel, C. G.; Kirollos, F. N.; Hussien, R. A. A.; Al-Mahallawi, A. M.; Sedeek, M. S. Chemical Composition and Potentiation of Insecticidal and Fungicidal Activities of Citrus Trifoliata L. Fruits Essential Oil against Spodoptera Littoralis, Fusarium Oxysporum and Fusarium Solani via Nano-Cubosomes. *Natural Product Research* **2021**, *35* (14), 2438−2443.
(50) Ibáñez, M. D.; Sanchez-Ballester, N. M.; Blázquez, M. A. Encapsulated Limonene: A Pleasant Lemon-like Aroma with Promising Application in the Agri-Food Industry. A Review. *Molecules* **2020**, *25* (11), 2598.
(51) Zhang, Z.; Vriesekoop, F.; Yuan, Q.; Liang, H. Effects of Nisin on the Antimicrobial Activity of D-Limonene and Its Nanoemulsion. *Food Chem.* **2014**, *150*, 307−312.
(52) Zahi, M. R.; El Hattab, M.; Liang, H.; Yuan, Q. Enhancing the Antimicrobial Activity of D-Limonene Nanoemulsion with the Inclusion of ε-Polylysine. *Food Chem.* **2017**, *221*, 18−23.
(53) Fagodia, S. K.; Singh, H. P.; Batish, D. R.; Kohli, R. K. Phytotoxicity and Cytotoxicity of Citrus Aurantiifolia Essential Oil and Its Major Constituents: Limonene and Citral. *Industrial Crops and Products* **2017**, *108* (May), 708−715.

https://doi.org/10.1021/acssuschemeng.3c02992
ACS Sustainable Chem. Eng. XXXX, XXX, XXX−XXX